

---

# Missing Data Imputation for Galaxy Redshift Estimation

---

Kieran J. Luken\*, Rabina Padhy, X. Rosalind Wang\*  
Western Sydney University, Penrith, NSW, Australia  
k.luken@westernsydney.edu.au  
rosalind.wang@westernsydney.edu.au

## Abstract

Astronomical data is full of holes. While there are many reasons for this missing data, the data can be randomly missing, caused by things like data corruptions or unfavourable observing conditions. We test some simple data imputation methods (Mean, Median, Minimum, Maximum and  $k$ -Nearest Neighbours (kNN)), as well as two more complex methods (Multivariate Imputation by using Chained Equation (MICE) and Generative Adversarial Imputation Network (GAIN)) against data where increasing amounts are randomly set to missing. We then use the imputed datasets to estimate the redshift of the galaxies, using the kNN and Random Forest ML techniques. We find that the MICE algorithm provides the lowest Root Mean Square Error and consequently the lowest prediction error, with the GAIN algorithm the next best.

## 1 Introduction

Astronomical data sets often contain missing values. There are many different causes for the missing values: In a single survey, data can be missing due to incomplete observations, recording problems, data corruptions, instrument limitations or unfavourable observing conditions. When multiple surveys are combined together, data can be missing due to varying survey depths, or that some objects are not present in one of the surveys. Traditionally, samples with missing values are either ignored or the values replaced with the mean or minimum/maximum of the data set. The former means a large fraction of the data are often ignored in a data analysis task for astronomical data sets. The latter introduces large errors in the missing value, and consequently errors in the analysed results.

With the growing popularity of deep learning, several deep learning methods for data imputation have been introduced in the literature (Pereira et al., 2020; Yoon et al., 2018; Shang et al., 2017; Lee et al., 2019) that take advantage of the generative nature of these methods. In this work, we investigate one of these methods, Generative Adversarial Imputation Network (GAIN; Yoon et al., 2018) — in an initial study on standard datasets, we found GAIN to be most computationally efficient among existing Generative Adversarial Network (GAN) based algorithms, with only a slight degradation on performance. For comparison, we contrast two other popular Machine Learning (ML) data imputation methods,  $k$ -Nearest Neighbours (kNN) and Multivariate Imputation by using Chained Equation (MICE; S. van Buuren, 2000).

We examine the effect of missing data imputation on redshift estimation. For most aspects of science, knowledge of an astronomical source’s redshift is an essential indicator of the distance and age of the source. Ideally, this redshift is measured directly using spectroscopy, however, for large astronomical surveys, spectroscopy data will not be available. Previously, Luken et al. (2021)<sup>1</sup> performed an

---

\* Authors also with Data61 CSIRO, NSW, Australia

<sup>1</sup>Available as a pre-print at [https://luken.dev/Papers/2021\\_ASCOM\\_Estimate\\_Redshift.pdf](https://luken.dev/Papers/2021_ASCOM_Estimate_Redshift.pdf)

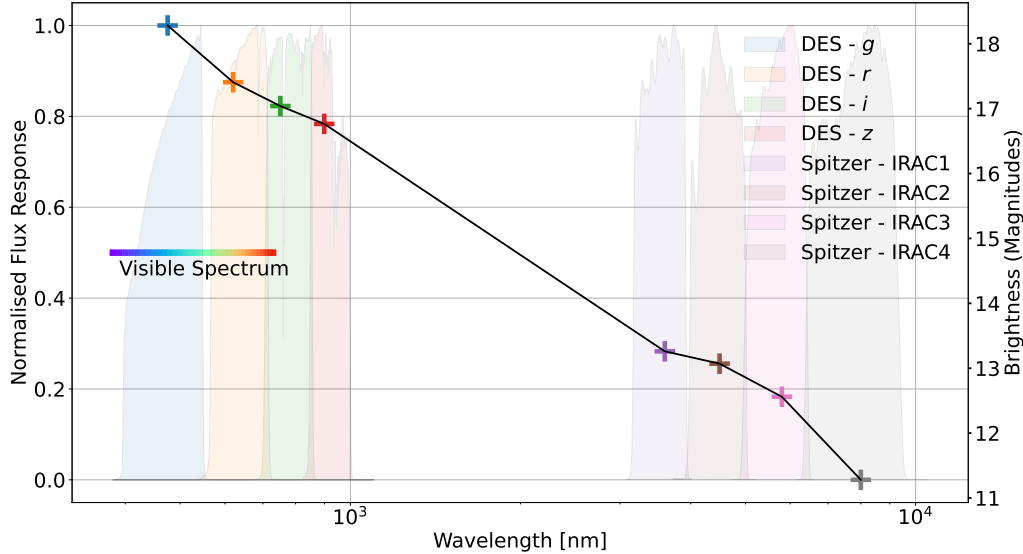


Figure (1) The SED of the extragalactic source ATLAS3\_J033402.4-281418C, taken from the ATLAS DR3. The background shows the filter coverage used by this work, with the “+” in the foreground representing the measured photometry at each band. The wavelengths being measured are along the x-axis, with the left-y-axis showing the normalised flux response of the filters being measured, and the right-y-axis showing the brightness of the source in each band.

in-depth study of using two popular ML methods to estimate the redshift of radio galaxies, where traditional redshift estimation techniques like template fitting have been shown to struggle (Norris et al., 2019). In this work, we investigate the accuracy of estimated redshift using imputed data at various missing rates, and compare their results against the estimation from non-imputed data.

## 2 Methods

### 2.1 Data set

This work uses the same data as that described in (Luken et al., 2021). The data set comprised of 1311 objects from the Australia Telescope Large Area Survey (ATLAS; Norris et al., 2006; Franzen et al., 2015) radio continuum catalogue. In addition to the radio flux measured using the Australia Telescope Compact Array, the data set contains spectroscopic redshift measurements (Yuan et al., 2015; Childress et al., 2017; Lidman et al., 2020) measured primarily using the Anglo-Australian Telescope,  $g$ ,  $r$ ,  $i$  and  $z$  optical magnitudes measured using the Dark Energy Camera at the Cerro Tololo Inter-American Observatory (Dark Energy Survey Collaboration et al., 2016), and 3.6, 4.5, 5.4 and 8.0  $\mu\text{m}$  infrared flux measurements measured using the Spitzer Space Telescope (Lonsdale et al., 2003). All attributes were standardised to  $\mathcal{N}(0, 1)$ . The data are available online<sup>2</sup>, with an example Spectral Energy Distribution (SED) demonstrated in Figure 1.

The data is partitioned randomly into two sets: using 70% of the full data set for training, and the remaining 30% as test data. We quantise the redshift values into 15 redshift bins for classification, with equal numbers of sources in each. The test data are used for both imputation and classification prediction. We applied different missing rates — 2%, 5%, 10%, 15%, 20%, 25% and 30% — to the test data, randomly removing a percentage of the data. The same imputed test data is then used for prediction using different classification methods. The experiment was repeated 100 times using different random seeds in order to estimate the variance in the results. This random sampling has the added effect of ensuring that the distributions of galaxies in the training and test sets are even.

<sup>2</sup><https://github.com/kluken/Redshift-kNN-2021>, GPL-3.0 License.

## 2.2 Data imputation algorithms

The simplest way for data imputation is to replace the missing value with a value of some summary statistics. In this work, we tested imputation with **mean**, **median**, **minimum** and **maximum** values of individual attributes. We calculate the median value for a data set with even number of samples as the mean between the two middle data points.

In *k*-Nearest Neighbours (kNN) data imputation, the distance between two samples are calculated using the features without missing values. Euclidean distance was used in this work. The missing values are imputed using the mean value from *k* nearest neighbours in the data set.

**Multivariate Imputation by using Chained Equation (MICE)** performs data imputation by filling the missing values multiple times. The algorithm initialises all missing value with the mean of their respective attribute. Each attribute’s missing values are then estimated as a regression problem using the other attributes in the data set as the independent variables. The cycle is repeated multiple times. We repeated the cycle 10 times, which is the general practice.

Finally, we tested **Generative Adversarial Imputation Network (GAIN)** (Yoon et al., 2018), where the generator’s aim is imputation, and the discriminator’s goal is to distinguish between observed and imputed components. The generator is designed to maximize the discriminator’s misclassification rate, whereas the discriminator’s aim is to minimize the classification loss. The GAIN architecture also provides the discriminator with additional information in the form of *hints*, which ensures that the generator generates samples according to the true underlying data distribution.

## 2.3 Machine learning algorithm

Luken et al. (2021) performed regression and classification on the data set using both kNN with three different distance metrics and Random Forest (RF) algorithms. These authors concluded that for this data set, kNN with Mahalanobis distance has the best regression and classification performances. Therefore, for this work, we concentrated our evaluation using this specific algorithm. We also evaluated the performance using RF as a comparison.

The kNN algorithm (Cover and Hart, 1967) computes a similarity matrix between all sources based on sample attributes through some distance metric. Using the similarity matrix, the kNN algorithm finds the  $k_N$  most similar sources (where  $k_N$  was optimised using  $k_f$ -fold cross-validation), and takes either the mean value (for regression) or the mode class (for classification) of the sources’ redshift as the estimated redshift for each source.

The Mahalanobis distance metric (Mahalanobis, 1936) normalises the variance and covariance of the input features by transforming the features using the inverse of the covariance matrix,  $S$ . The Mahalanobis distance,  $d(\vec{p}, \vec{q})$  between two feature vectors  $\vec{p}$  and  $\vec{q}$  is:

$$d(\vec{p}, \vec{q}) = \sqrt{(\vec{p} - \vec{q})^T S^{-1} (\vec{p} - \vec{q})}. \quad (1)$$

The value of  $k_N$  used in the kNN in this work is optimised using  $k$ -fold (where  $k$  is hereafter  $k_f$  and is set to 10 for this work) cross-validation. For regression, we tested all integer values of  $k_N$  between 3 and 23, and for classification we tested all odd integer values between 3 and 43.

RF (Morgan and Sonquist, 1963) is an ensemble ML method, where a set of Decision Tree (DT) are built through bootstrapping. Each DT is given a slightly different training data. This leads to a diversity of trees in the ensemble, which contribute to robustness of the model as a whole. The optimum number of trees is determined through  $k$ -fold cross-validation.

## 2.4 Performance metrics

The error metric used for imputation performance is Root Mean Square Error (RMSE). To calculate the RMSE, we mask out any data points in the test data set that is not a missing value, and only calculate the difference between the predicted value and the actual value.

The primary error metric for the redshift estimation is the  $\eta_{0.15}$  outlier rate:

$$\eta_{0.15} = \frac{\text{count}(|z_{spec} - z_{photo}| > 0.15 \times (1 + z_{spec}))}{\text{Number Of Sources}}, \quad (2)$$

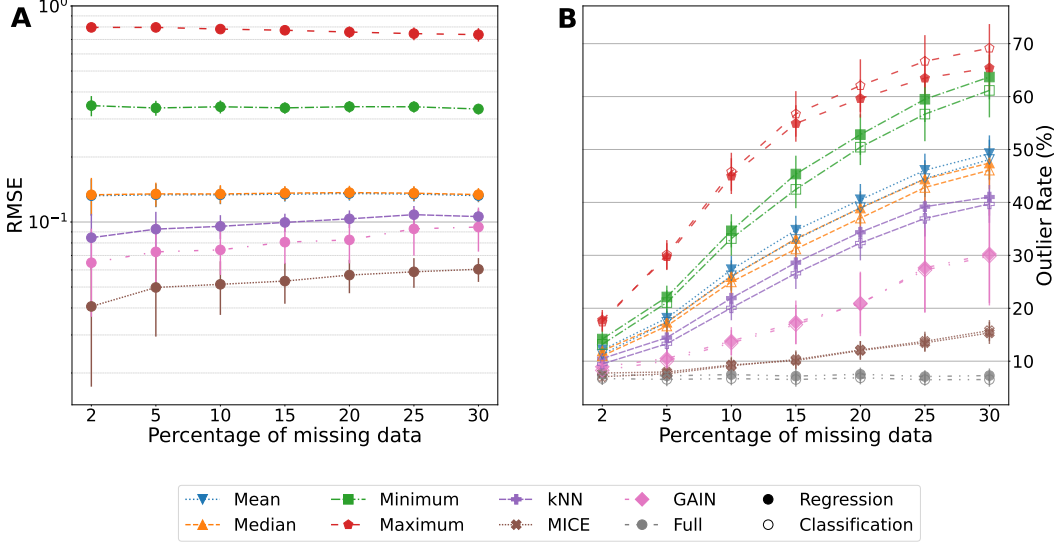


Figure (2) Results at different percentages of missing data. (A) The RMSE of each of the imputation methods. The y-axis is in log scale to emphasize the different results. (B) The outlier rate (defined in Equation 2) of the kNN Regression (filled markers) and Classification (hollow markers), tested on the different datasets created by the different imputation methods on the test data. Also shown on B is the outlier rate using the test set without missing data. All markers are set to the mean of the test, with error bars representing  $\pm 1$  standard deviation.

where  $z_{spec}$  is the estimated redshift and  $z_{photo}$  is the measured redshift of a source. The  $\eta_{0.15}$  outlier rate is a percentage representing the number of ‘catastrophic failures’, and is commonly found in literature (Luken et al., 2021, and references therein).

## 2.5 Software

This work makes use of the *Scikit-learn* Python package (Pedregosa et al., 2011) for the implementation of kNN algorithms. We also used MICE<sup>3</sup> and GAIN<sup>4</sup> implementations from GitHub. The code used in this work is available on Github<sup>5</sup>

## 3 Results

### 3.1 Imputation Results

Error rates of the imputed datasets at different missing rates are shown in Figure2A. All tests show the same trend over the different missing rates. This is due to the training method utilised – the training/test split was completed before the test data were blanked. Therefore, the training data remains the same for all tests, ensuring that differences in the final prediction errors quoted are entirely due to the missing data in the test sample, and not potentially contaminated by errors in the training set as well.

The MICE algorithm performs best (RMSE  $\approx 0.05 \pm 0.01$ ) across all missing rates, followed by the GAIN (RMSE  $\approx 0.08 \pm 0.02$ ) and kNN (RMSE  $\approx 0.1 \pm 0.01$ ) algorithms. The simple Mean (RMSE  $\approx 0.13 \pm 0.01$ ), Median (RMSE  $\approx 0.14 \pm 0.01$ ), Minimum (RMSE  $\approx 0.34 \pm 0.02$ ) and Maximum (RMSE  $\approx 0.77 \pm 0.04$ ) imputation all perform progressively worse.

<sup>3</sup>[https://github.com/farrajota/benchmark\\_mice\\_algorithms](https://github.com/farrajota/benchmark_mice_algorithms), MIT License.

<sup>4</sup><https://github.com/jsyoon0823/GAIN>, Apache License, Version 2.0.

<sup>5</sup>[https://github.com/kluken/Redshift\\_Imputation](https://github.com/kluken/Redshift_Imputation), GPL-3.0 License.

The opposite was true for the time taken<sup>6</sup>, where at 15% missing data rate, the Mean, Median, Minimum and Maximum were imputed effectively instantly, followed by the kNN algorithm ( $\approx 1.69 \pm 1.12$  s), GAIN algorithm ( $\approx 123.86 \pm 11.55$  s), and MICE algorithm ( $\approx 871.6 \pm 202.68$  s).

### 3.2 Prediction Results

Figure 2B (Right) shows the prediction error (the Outlier Rate, defined in Equation 2) using kNN. Results using RF have similar trend, hence omitted here for brevity. At low missing rates (2–5%), the outlier rates are similar to the baseline using imputed data from MICE and GAIN, although higher levels of missing data result in higher outlier rates.

The prediction error follows the imputation results – the lowest outlier rates are achieved using datasets where the imputation methods achieved the lowest RMSE. In all cases, the classification outlier rates very closely followed the regression outlier rates, with the classification outlier rates often being marginally lower, although well within the error bars.

Looking at classification-based models predicting the datasets where 15% of the test set was set to missing, which has a baseline of  $6.54 \pm 1.36\%$ . The MICE-imputed dataset performed best ( $10.31 \pm 1.72\%$ ), followed by the GAIN-imputed dataset ( $16.9 \pm 3.72\%$ ) and kNN-imputed dataset ( $26.6 \pm 2.95\%$ ). As with the imputation results, the Median ( $31.19 \pm 2.84\%$ ), Mean ( $32.99 \pm 2.85\%$ ), Minimum ( $42.46 \pm 3.56\%$ ) and Maximum ( $56.72 \pm 4.31\%$ ) datasets performed the worst.

## 4 Conclusion and Future Work

Astronomical surveys are of most use when their catalogues are cross-matched with other surveys at different wavelengths. However, most astronomical surveys contain missing data for a variety of reasons, including brightness limits or issues/errors recording data for some reason. While the former is common, this work only looks at the case where data is missing at random – where the data has not been able to be recorded correctly. Future work will look at the case where astronomical sources are too faint to be seen at particular wavelengths, and will look at including additional data where the redshift is not known.

This work finds that in this case, the MICE algorithm performs best at recovering the missing values, resulting in both a lower RMSE and final outlier rate. Using the MICE algorithm results in acceptable redshift estimates (where  $\approx 10\%$  of the estimates are defined as outliers) where up to 15% of the data is missing. The GAIN algorithm has potential with slightly higher prediction errors but at 1/7 the running time for the imputation. However, it likely under-performed due to the small sample size. The kNN algorithm and other simple methods performed poorly in both imputation error and most importantly redshift estimation error, and should not be used going forward.

Future work will include incorporating alternative training methods, including training on imputed data, and training including astronomical sources without a measured redshift, and testing the imputation methods on datasets containing real missing values.

## Acknowledgments and Disclosure of Funding

The Australia Telescope Compact Array is part of the Australia Telescope National Facility which is funded by the Australian Government for operation as a National Facility managed by CSIRO. We acknowledge the Gomeri people as the traditional owners of the Observatory site.

Based in part on data acquired at the Anglo-Australian Telescope. We acknowledge the traditional owners of the land on which the AAT stands, the Gamilaroi people, and pay our respects to elders past and present.

This work is based on archival data obtained with the Spitzer Space Telescope, which was operated by the Jet Propulsion Laboratory, California Institute of Technology under a contract with NASA. Support for this work was provided by an award issued by JPL/Caltech

This project used public archival data from the Dark Energy Survey (DES). Funding for the DES Projects has been provided by the U.S. Department of Energy, the U.S. National Science Foundation,

---

<sup>6</sup>All tests were completed on a desktop computer with an AMD Ryzen 7 1700 CPU and 16GB RAM

the Ministry of Science and Education of Spain, the Science and Technology Facilities Council of the United Kingdom, the Higher Education Funding Council for England, the National Center for Supercomputing Applications at the University of Illinois at Urbana-Champaign, the Kavli Institute of Cosmological Physics at the University of Chicago, the Center for Cosmology and Astro-Particle Physics at the Ohio State University, the Mitchell Institute for Fundamental Physics and Astronomy at Texas A&M University, Financiadora de Estudos e Projetos, Fundação Carlos Chagas Filho de Amparo à Pesquisa do Estado do Rio de Janeiro, Conselho Nacional de Desenvolvimento Científico e Tecnológico and the Ministério da Ciência, Tecnologia e Inovação, the Deutsche Forschungsgemeinschaft, and the Collaborating Institutions in the Dark Energy Survey.

The Collaborating Institutions are Argonne National Laboratory, the University of California at Santa Cruz, the University of Cambridge, Centro de Investigaciones Energéticas, Medioambientales y Tecnológicas-Madrid, the University of Chicago, University College London, the DES-Brazil Consortium, the University of Edinburgh, the Eidgenössische Technische Hochschule (ETH) Zürich, Fermi National Accelerator Laboratory, the University of Illinois at Urbana-Champaign, the Institut de Ciències de l’Espai (IEEC/CSIC), the Institut de Física d’Altes Energies, Lawrence Berkeley National Laboratory, the Ludwig-Maximilians Universität München and the associated Excellence Cluster Universe, the University of Michigan, the National Optical Astronomy Observatory, the University of Nottingham, The Ohio State University, the OzDES Membership Consortium, the University of Pennsylvania, the University of Portsmouth, SLAC National Accelerator Laboratory, Stanford University, the University of Sussex, and Texas A&M University.

Based in part on observations at Cerro Tololo Inter-American Observatory, National Optical Astronomy Observatory, which is operated by the Association of Universities for Research in Astronomy (AURA) under a cooperative agreement with the National Science Foundation.

## References

- Childress, M. J., Lidman, C., Davis, T. M., Tucker, B. E., Asorey, J., Yuan, F., Abbott, T. M. C., Abdalla, F. B., Allam, S., Annis, J., Banerji, M., Benoit-Lévy, A., Bernard, S. R., Bertin, E., Brooks, D., Buckley-Geer, E., Burke, D. L., Carnero Rosell, A., Carollo, D., Carrasco Kind, M., Carretero, J., Castander, F. J., Cunha, C. E., da Costa, L. N., D’Andrea, C. B., Doel, P., Eifler, T. F., Evrard, A. E., Flaugher, B., Foley, R. J., Fosalba, P., Frieman, J., García-Bellido, J., Glazebrook, K., Goldstein, D. A., Gruen, D., Gruendl, R. A., Gschwend, J., Gupta, R., Gutierrez, G., Hinton, S. R., Hoormann, J. K., James, D. J., Kessler, R., Kim, A. G., King, A. L., Kovacs, E., Kuehn, K., Kuhlmann, S., Kuropatkin, N., Lagattuta, D. J., Lewis, G. F., Li, T. S., Lima, M., Lin, H., Macaulay, E., Maia, M. A. G., Marriner, J., March, M., Marshall, J. L., Martini, P., McMahon, R. G., Menanteau, F., Miquel, R., Moller, A., Morganson, E., Mould, J., Mudd, D., Muthukrishna, D., Nichol, R. C., Nord, B., Ogando, R. L. C., Ostrovski, F., Parkinson, D., Plazas, A. A., Reed, S. L., Reil, K., Romer, A. K., Rykoff, E. S., Sako, M., Sanchez, E., Scarpine, V., Schindler, R., Schubnell, M., Scolnic, D., Sevilla-Noarbe, I., Seymour, N., Sharp, R., Smith, M., Soares-Santos, M., Sobreira, F., Sommer, N. E., Spinka, H., Suchyta, E., Sullivan, M., Swanson, M. E. C., Tarle, G., Uddin, S. A., Walker, A. R., Wester, W., and Zhang, B. R. (2017). OzDES multifibre spectroscopy for the Dark Energy Survey: 3-yr results and first data release. *Monthly Notices of the Royal Astronomical Society*, 472(1):273–288.
- Cover, T. and Hart, P. (1967). Nearest neighbor pattern classification. *IEEE Transactions on Information Theory*, 13(1):21–27.
- Dark Energy Survey Collaboration, Abbott, T., Abdalla, F. B., Aleksić, J., Allam, S., Amara, A., Bacon, D., Balbinot, E., Banerji, M., Bechtol, K., Benoit-Lévy, A., Bernstein, G. M., Bertin, E., Blazek, J., Bonnett, C., Bridle, S., Brooks, D., Brunner, R. J., Buckley-Geer, E., Burke, D. L., Caminha, G. B., Capozzi, D., Carlsen, J., Carnero-Rosell, A., Carollo, M., Carrasco-Kind, M., Carretero, J., Castander, F. J., Clerkin, L., Collett, T., Conselice, C., Croce, M., Cunha, C. E., D’Andrea, C. B., da Costa, L. N., Davis, T. M., Desai, S., Diehl, H. T., Dietrich, J. P., Dodelson, S., Doel, P., Drlica-Wagner, A., Estrada, J., Etherington, J., Evrard, A. E., Fabbri, J., Finley, D. A., Flaugher, B., Foley, R. J., Fosalba, P., Frieman, J., García-Bellido, J., Gaztanaga, E., Gerdes, D. W., Giannantonio, T., Goldstein, D. A., Gruen, D., Gruendl, R. A., Guarnieri, P., Gutierrez, G., Hartley, W., Honscheid, K., Jain, B., James, D. J., Jeltema, T., Jouvel, S., Kessler, R., King, A., Kirk, D., Kron, R., Kuehn, K., Kuropatkin, N., Lahav, O., Li, T. S., Lima, M., Lin, H., Maia, M. A. G., Makler, M., Manera, M., Maraston, C., Marshall, J. L., Martini, P., McMahon, R. G.,

- Melchior, P., Merson, A., Miller, C. J., Miquel, R., Mohr, J. J., Morice-Atkinson, X., Naidoo, K., Neilsen, E., Nichol, R. C., Nord, B., Ogando, R., Ostrovski, F., Palmese, A., Papadopoulos, A., Peiris, H. V., Peoples, J., Percival, W. J., Plazas, A. A., Reed, S. L., Refregier, A., Romer, A. K., Roodman, A., Ross, A., Roza, E., Rykoff, E. S., Sadeh, I., Sako, M., Sánchez, C., Sanchez, E., Santiago, B., Scarpine, V., Schubnell, M., Sevilla-Noarbe, I., Sheldon, E., Smith, M., Smith, R. C., Soares-Santos, M., Sobreira, F., Soumagnac, M., Suchyta, E., Sullivan, M., Swanson, M., Tarle, G., Thaler, J., Thomas, D., Thomas, R. C., Tucker, D., Vieira, J. D., Vikram, V., Walker, A. R., Wechsler, R. H., Weller, J., Wester, W., Whiteway, L., Wilcox, H., Yanny, B., Zhang, Y., and Zuntz, J. (2016). The Dark Energy Survey: more than dark energy - an overview. *Monthly Notices of the Royal Astronomical Society*, 460:1270–1299.
- Franzen, T. M. O., Banfield, J. K., Hales, C. A., Hopkins, A., Norris, R. P., Seymour, N., Chow, K. E., Herzog, A., Huynh, M. T., Lenc, E., Mao, M. Y., and Middelberg, E. (2015). ATLAS - I. Third release of 1.4 GHz mosaics and component catalogues. *Monthly Notices of the Royal Astronomical Society*, 453:4020–4036.
- Lee, D., Kim, J., Moon, W.-J., and Ye, J. C. (2019). Collagan: Collaborative gan for missing image data imputation. In *Proceedings of the IEEE/CVF Conference on Computer Vision and Pattern Recognition*, pages 2487–2496.
- Lidman, C., Tucker, B. E., Davis, T. M., Uddin, S. A., Asorey, J., Bolejko, K., Brout, D., Calcino, J., Carollo, D., Carr, A., Childress, M., Hoormann, J. K., Foley, R. J., Galbany, L., Glazebrook, K., Hinton, S. R., Kessler, R., Kim, A. G., King, A., Kremin, A., Kuehn, K., Lagattuta, D., Lewis, G. F., Macaulay, E., Malik, U., March, M., Martini, P., Möller, A., Mudd, D., Nichol, R. C., Panther, F., Parkinson, D., Pursiainen, M., Sako, M., Swann, E., Scalzo, R., Scolnic, D., Sharp, R., Smith, M., Sommer, N. E., Sullivan, M., Webb, S., Wiseman, P., Yu, Z., Yuan, F., Zhang, B., Abbott, T. M. C., Aguena, M., Allam, S., Annis, J., Avila, S., Bertin, E., Bhargava, S., Brooks, D., Carnero Rosell, A., Carrasco Kind, M., Carretero, J., Castander, F. J., Costanzi, M., da Costa, L. N., De Vicente, J., Doel, P., Eifler, T. F., Everett, S., Fosalba, P., Frieman, J., García-Bellido, J., Gaztanaga, E., Gruen, D., Gruendl, R. A., Gschwend, J., Gutierrez, G., Hartley, W. G., Hollowood, D. L., Honscheid, K., James, D. J., Kuropatkin, N., Li, T. S., Lima, M., Lin, H., Maia, M. A. G., Marshall, J. L., Melchior, P., Menanteau, F., Miquel, R., Palmese, A., Paz-Chinchón, F., Plazas, A. A., Roodman, A., Rykoff, E. S., Sanchez, E., Santiago, B., Scarpine, V., Schubnell, M., Serrano, S., Sevilla-Noarbe, I., Suchyta, E., Swanson, M. E. C., Tarle, G., Tucker, D. L., Varga, T. N., Walker, A. R., Wester, W., Wilkinson, R. D., and DES Collaboration (2020). OzDES multi-object fibre spectroscopy for the Dark Energy Survey: results and second data release. *Monthly Notices of the Royal Astronomical Society*, 496(1):19–35.
- Lonsdale, C. J., Smith, H. E., Rowan-Robinson, M., Surace, J., Shupe, D., Xu, C., Oliver, S., Padgett, D., Fang, F., Conrow, T., Franceschini, A., Gautier, N., Griffin, M., Hacking, P., Masci, F., Morrison, G., O’Linger, J., Owen, F., Pérez-Fournon, I., Pierre, M., Puetter, R., Stacey, G., Castro, S., Polletta, M. d. C., Farrah, D., Jarrett, T., Frayer, D., Siana, B., Babbedge, T., Dye, S., Fox, M., Gonzalez-Solares, E., Salaman, M., Berta, S., Condon, J. J., Dole, H., and Serjeant, S. (2003). SWIRE: The SIRTf Wide-Area Infrared Extragalactic Survey. *Publications of the Astronomical Society of the Pacific*, 115:897–927.
- Luken, K. J., Norris, R. P., Wang, X. R., Park, L. A. F., and Filipovic, M. D. (2021). Estimating galaxy redshift in radio-selected datasets using machine learning. "[https://luken.dev/Papers/2021\\_ASCOM\\_Estimate\\_Redshift.pdf](https://luken.dev/Papers/2021_ASCOM_Estimate_Redshift.pdf)". under review.
- Mahalanobis, P. C. (1936). On the generalized distance in statistics. In *On the Generalised Distance in Statistics*. National Institute of Science of India.
- Morgan, J. N. and Sonquist, J. A. (1963). Problems in the Analysis of Survey Data, and a Proposal. *Journal of the American Statistical Association*, 58(302):415–434.
- Norris, R. P., Afonso, J., Appleton, P. N., Boyle, B. J., Ciliegi, P., Croom, S. M., Huynh, M. T., Jackson, C. A., Koekemoer, A. M., Lonsdale, C. J., Middelberg, E., Mobasher, B., Oliver, S. J., Polletta, M., Siana, B. D., Smail, I., and Voronkov, M. A. (2006). Deep ATLAS Radio Observations of the Chandra Deep Field-South/Spitzer Wide-Area Infrared Extragalactic Field. *Astronomical Journal*, 132:2409–2423.

- Norris, R. P., Salvato, M., Longo, G., Brescia, M., Budavari, T., Carliles, S., Cavuoti, S., Farrah, D., Geach, J., Luken, K., Musaeva, A., Polsterer, K., Riccio, G., Seymour, N., Smolčić, V., Vaccari, M., and Zinn, P. (2019). A Comparison of Photometric Redshift Techniques for Large Radio Surveys. *Publications of the Astronomical Society of the Pacific*, 131(1004):108004.
- Pedregosa, F., Varoquaux, G., Gramfort, A., Michel, V., Thirion, B., Grisel, O., Blondel, M., Prettenhofer, P., Weiss, R., Dubourg, V., Vanderplas, J., Passos, A., Cournapeau, D., Brucher, M., Perrot, M., and Duchesnay, E. (2011). Scikit-learn: Machine Learning in Python. *Journal of Machine Learning Research*, 12:2825–2830.
- Pereira, R. C., Santos, M. S., Rodrigues, P. P., and Abreu, P. H. (2020). Reviewing autoencoders for missing data imputation: Technical trends, applications and outcomes. *Journal of Artificial Intelligence Research*, 69:1255–1285.
- S. van Buuren, C. O. (2000). *Multivariate Imputation by Chained Equations*. Public Health, Netherlands.
- Shang, C., Palmer, A., Sun, J., Chen, K.-S., Lu, J., and Bi, J. (2017). Vigan: Missing view imputation with generative adversarial networks. In *2017 IEEE International Conference on Big Data (Big Data)*, pages 766–775. IEEE.
- Yoon, J., Jordon, J., and Schaar, M. (2018). GAIN: Missing data imputation using generative adversarial nets. In *International Conference on Machine Learning*, pages 5689–5698. PMLR.
- Yuan, F., Lidman, C., Davis, T. M., Childress, M., Abdalla, F. B., Banerji, M., Buckley-Geer, E., Camero Rosell, A., Carollo, D., Castander, F. J., D’Andrea, C. B., Diehl, H. T., Cunha, C. E., Foley, R. J., Frieman, J., Glazebrook, K., Gschwend, J., Hinton, S., Jouvel, S., Kessler, R., Kim, A. G., King, A. L., Kuehn, K., Kuhlmann, S., Lewis, G. F., Lin, H., Martini, P., McMahon, R. G., Mould, J., Nichol, R. C., Norris, R. P., O’Neill, C. R., Ostrovski, F., Papadopoulos, A., Parkinson, D., Reed, S., Romer, A. K., Rooney, P. J., Rozo, E., Rykoff, E. S., Sako, M., Scalzo, R., Schmidt, B. P., Scolnic, D., Seymour, N., Sharp, R., Sobreira, F., Sullivan, M., Thomas, R. C., Tucker, D., Uddin, S. A., Wechsler, R. H., Wester, W., Wilcox, H., Zhang, B., Abbott, T., Allam, S., Bauer, A. H., Benoit-Lévy, A., Bertin, E., Brooks, D., Burke, D. L., Carrasco Kind, M., Covarrubias, R., Croce, M., da Costa, L. N., DePoy, D. L., Desai, S., Doel, P., Eifler, T. F., Evrard, A. E., Fausti Neto, A., Flaugher, B., Fosalba, P., Gaztanaga, E., Gerdes, D., Gruen, D., Gruendl, R. A., Honscheid, K., James, D., Kuropatkin, N., Lahav, O., Li, T. S., Maia, M. A. G., Makler, M., Marshall, J., Miller, C. J., Miquel, R., Ogando, R., Plazas, A. A., Roodman, A., Sanchez, E., Scarpine, V., Schubnell, M., Sevilla-Noarbe, I., Smith, R. C., Soares-Santos, M., Suchyta, E., Swanson, M. E. C., Tarle, G., Thaler, J., and Walker, A. R. (2015). OzDES multifibre spectroscopy for the Dark Energy Survey: first-year operation and results. *Monthly Notices of the Royal Astronomical Society*, 452(3):3047–3063.